

# Superscaling analysis of quasielastic electron scattering with relativistic effective mass

J.E. Amaro,<sup>1,\*</sup> E. Ruiz Arriola,<sup>1,†</sup> and I. Ruiz Simo<sup>1,‡</sup>

<sup>1</sup>*Departamento de Física Atómica, Molecular y Nuclear  
and Instituto Carlos I de Física Teórica y Computacional  
Universidad de Granada, E-18071 Granada, Spain.*

(Dated: January 20, 2017)

We provide a parametrization of a new phenomenological scaling function obtained from a chi-square fit to a selected set of  $(e,e')$  cross section data expanding a band centered around the quasielastic peak. We start from a re-analysis of quasielastic electron scattering from nuclear matter within the relativistic mean field model. The cross section depends on the relativistic effective mass of the nucleon,  $m_N^*$ , and it scales with respect to a new scaling variable,  $\psi^*$ . This suggests a new superscaling approach with effective mass (SuSAM\*) for predicting quasielastic cross sections within an uncertainty band. The model reproduces previously established results on the enhancement of the transverse response function as compared to the traditional relativistic Fermi gas.

## INTRODUCTION

The description of quasielastic electron scattering cross section is still an open problem in theoretical nuclear physics. The recent neutrino experiments with accelerators have emphasized the importance of a global precise description of lepton scattering from nuclei at intermediate energies [1–5]. Although a great deal of progress has been achieved with models based on first principles description of the nuclear system [6], alternative approaches based on the spectral function [7, 8] or the shell model [9], to mention some recent studies, have been put forward. As a general rule, the models cannot provide yet a complete description of the whole set of  $(e, e')$  data at the full range of kinematics needed, specially for high momentum and energy transfers, where a relativistic description becomes mandatory [10, 11]. Not to mention that there are still basic issues like gauge invariance that are not easy to control and generate well known ambiguities.

In addition to the relativistic corrections in the kinematics and in the current operator, the importance of relativistic corrections stemming from the dynamics has been emphasized from a fully relativistic mean field calculation [12]. In those studies the combination of scalar and vector relativistic potentials naturally produce an enhancement of the lower components of relativistic nucleon wave functions [13] and correspondingly an enhancement of the transverse response function. This is a genuine relativistic dynamical effect, and it goes away, for example, after a semirelativistic approximation where the lower components are neglected or projected out [11]. It is known that the transverse cross section is larger than the predictions of the independent nucleon model. While the transverse enhancement has primarily been attributed to multi-nucleon processes via meson-exchange currents and  $\Delta$  excitation [14], it should be noted that this enhancement can also be regarded partly as due to relativity.

A major difficulty in the description of the inclusive

$(e, e')$  cross section is that it is the result of contributions from many unseen processes and interferences that cannot be disentangled easily. From simplistic viewpoint the cross section can be regarded as the sum of nucleon knockout plus multinucleon knockout plus pion-nucleon emission plus additional inelastic processes in the deep region. Both 1p-1h and  $1\pi$ 1p-1h are contaminated by 2p-2h and cannot be unambiguously separated from it [15–17]. From the theoretical point of view the one-nucleon knockout process generates the quasielastic peak. But experimentally this peak can only be isolated from the data of the longitudinal response function for moderate momentum transfer where meson-exchange currents and pion emission are predominantly transverse [18, 19].

Scaling ideas have prompted studies which are promising phenomenological alternatives complementary to the theoretical microscopic models [20]. The superscaling approach (SuSA) [18, 19, 21, 22] exploited the scaling properties of the reduced longitudinal response function (divided by the corresponding single-nucleon structure function) when plotted against an appropriate scaling variable  $\psi'$ . This allowed to implement a phenomenological longitudinal scaling function  $f_L(\psi')$  fitted to electron data. This scaling function embodies implicitly all the genuinely quasielastic nuclear physics processes. Thus any model aiming to describe the quasielastic reaction should be able to describe  $f_L$ .

All the processes violating scaling contribute mainly to the transverse response. Within the SuSA approach the “quasielastic” part of the transverse response function was computed by assuming the same scaling properties as the longitudinal response, and that a transverse (unknown) scaling function  $f_T$  exists. In the original SuSA approach it was simply assumed that  $f_T = f_L$  [22] and this allowed to construct a manageable model to predict neutrino cross sections from the  $(e, e')$  data. Although such an assumption was not based on data, semirelativistic models like that of ref. [11] give in fact  $f_T \simeq f_L$ .

The relativistic mean field (RMF) framework to finite

nuclei reproduces the experimental  $f_L$  function rather well and therefore this model can be used to test the validity of the  $f_T = f_L$  assumption under relativistic dynamics. This model is based on the Dirac-Hartree approximation of ref. [23]. In [12] it was actually found that in the RMF model  $f_T > f_L$ ; the precise value of  $f_T$  depends on the treatment of the off-shell ambiguities of the current operator. Under the CC2 prescription of de Forest [24],  $f_T$  is about 20% larger than  $f_L$ , while it is almost twice as large for CC1 [12]. The CC2 results for the  $(e, e')$  cross section seem more reasonable, and so this was the prescription used in the recent upgrade SuSA-v2 [25]. This new model includes nuclear effects which are theoretically-inspired by the RMF by using a transverse scaling function  $f_T$  which is different from  $f_L$ , and that also has an additional dependence on the momentum transfer  $q$ . Therefore the SuSA-v2 results do not scale anymore, although the model conserves the 'scaling' name by tradition.

In this work we explore a new scaling approach to describe, in a wide kinematical range, the  $(e, e')$  data by minimizing undesirable contaminations from inelastic scattering or other effects beyond the quasielastic conditions. We proceed by exploiting the scaling formalism and, at the same time, the proved good properties of the relativistic mean field, which already includes by construction the transverse response enhancement. Our goal is to return to the description of the quasielastic peak with only one phenomenological scaling function,  $f^*(\psi^*)$ , by fitting a subset of conveniently selected data. Thus, we expect that the double differential cross section improves over the SuSA model [18, 25]. We remind that the description of the SuSA model is not fully satisfactory because only the longitudinal response function was fitted and not the cross section. The SuSAv2 was an improvement by using a theoretical transverse scaling function coming from the RMF but at the cost of violating scaling [25]. In our approach, however, we maintain the scaling with respect to a new scaling variable  $\psi^*$  to be defined shortly.

In a previous work [26] we started exploring the  $\psi^*$  scaling idea in the context of the RMF for nuclear matter. In that study we obtained the best value of the effective mass

$$M^* = \frac{m_N^*}{m_N} = 0.8. \quad (1)$$

This value provides the best scaling behavior of the data with a large fraction of data concentrated around the universal scaling function of the relativistic Fermi gas

$$f_{\text{RFG}}(\psi^*) = \frac{3}{4}(1 - \psi^{*2})\theta(1 - \psi^{*2}) \quad (2)$$

The  $\psi^*$  variable was inspired by the mean field theory, that provides a reasonable description of the quasielastic response function [27, 28]. In the interacting RFG

the vector and scalar potentials generate an effective mass  $m_N^*$  for the nucleon in the medium. Our present approach, called SuSAM\* (super scaling approach with  $M^*$ ), enjoys the good features of the RMF in nuclear matter. It keeps gauge invariance (that SuSA violates because it introduces an energy shift to account for separation energy) and describes the dynamical enhancement of both the lower components of the relativistic spinors and the transverse response function.

In ref. [26] the effective mass was randomly modified around the mean value  $0.8 \pm 0.1$ , approximately simulating the dispersion band of the real data. In the present work we instead fit a selection of experimental data which are considered "true" quasielastic based on a data density criterium. Our main goal is to provide a simple fit of the new phenomenological  $\psi^*$ -scaling function,  $f^*(\psi^*)$  as the sum of two Gaussian functions, and similar fits for the dispersion band as well. This simple formula allows to predict the quasielastic cross section for arbitrary kinematics together with a uncertainty band, providing the maximum information from the scaling properties of the available  $(e, e')$  data, with few parameters. The uncertainty bands describe about 1000 "quasielastic" data out of the  $\sim 2500$  existing data for  $^{12}\text{C}$ . The data that lie outside the uncertainty band, are those generated by inelastic processes or low energy nuclear effects that break scaling explicitly.

## FORMALISM

We follow the notation introduced in Ref. [26]. We assume that an incident electron scatters off a nucleus transferring momentum  $\mathbf{q}$  and energy  $\omega$

The quasielastic cross section is

$$\frac{d\sigma}{d\Omega' d\epsilon'} = \sigma_{\text{Mott}} \{v_L R_L + v_T R_T\} \quad (3)$$

where  $\sigma_{\text{Mott}}$  is the Mott cross section, and  $\theta$  the scattering angle.  $R_L(q, \omega)$  and  $R_T(q, \omega)$  are the nuclear longitudinal and transverse response functions, respectively. The four-momentum transfer is  $Q^2 = \omega^2 - q^2 < 0$ . Finally the kinematical factors  $v_L, v_T$  are defined by

$$v_L = \frac{Q^4}{q^4} \quad (4)$$

$$v_T = \tan^2 \frac{\theta}{2} - \frac{Q^2}{2q^2}. \quad (5)$$

## RMF in nuclear matter

The SuSAM\* model is inspired by the RMF in nuclear matter which we summarize here. In this model we consider single-nucleon excitations with initial nucleon energy  $E = \sqrt{\mathbf{p}^2 + m_N^{*2}}$  in the mean field. The final

momentum of the nucleon is  $\mathbf{p}' = \mathbf{p} + \mathbf{q}$  and its energy is  $E' = \sqrt{\mathbf{p}'^2 + m_N^{*2}}$ . Note that initial and final nucleons have the same effective mass  $m_N^*$ . The Fermi momentum  $k_F = 225 \text{ MeV}/c$  for  $^{12}\text{C}$ . The nuclear response functions can be written in the factorized form for  $K = L, T$

$$R_K = r_K f^*(\psi^*), \quad (6)$$

where  $r_L$  and  $r_T$  are the single-nucleon contribution, taking into account the Fermi motion

$$r_K = \frac{\xi_F}{m_N^* \eta_F^3 \kappa} (ZU_K^p + NU_K^n) \quad (7)$$

and  $f^*(\psi^*)$  is the scaling function, given by Eq. (2). It depends only on the new scaling variable  $\psi^*$ , that is the minimum kinetic energy of the initial nucleon divided by the kinetic Fermi energy. The minimum energy allowed for a nucleon inside the nucleus to absorb the virtual photon (in units of  $m_N^*$ ) is

$$\epsilon_0 = \text{Max} \left\{ \kappa \sqrt{1 + \frac{1}{\tau}} - \lambda, \epsilon_F - 2\lambda \right\}, \quad (8)$$

where we have introduced the dimensionless variables

$$\lambda = \omega/2m_N^*, \quad (9)$$

$$\kappa = q/2m_N^*, \quad (10)$$

$$\tau = \kappa^2 - \lambda^2, \quad (11)$$

$$\eta_F = k_F/m_N^*, \quad (12)$$

$$\xi_F = \sqrt{1 + \eta_F^2} - 1, \quad (13)$$

$$\epsilon_F = \sqrt{1 + \eta_F^2}, \quad (14)$$

Usually [20] these variables are defined dividing by the nucleon mass  $m_N$  instead of  $m_N^*$ . The definition of the scaling variable is

$$\psi^* = \sqrt{\frac{\epsilon_0 - 1}{\epsilon_F - 1}} \text{sgn}(\lambda - \tau) \quad (15)$$

$\psi^*$  is negative to the left of the quasielastic peak ( $\lambda < \tau$ ) and positive on the right side.

The single nucleon response functions are

$$U_L = \frac{\kappa^2}{\tau} \left[ (G_E^*)^2 + \frac{(G_E^*)^2 + \tau(G_M^*)^2}{1 + \tau} \Delta \right] \quad (16)$$

$$U_T = 2\tau(G_M^*)^2 + \frac{(G_E^*)^2 + \tau(G_M^*)^2}{1 + \tau} \Delta \quad (17)$$

where the quantity  $\Delta$  has been introduced

$$\Delta = \frac{\tau}{\kappa^2} \xi_F (1 - \psi^{*2}) \left[ \kappa \sqrt{1 + \frac{1}{\tau}} + \frac{\xi_F}{3} (1 - \psi^{*2}) \right]. \quad (18)$$

One of the consequences of the present RMF approach is that the electric and magnetic form factors, are modified

in the medium due to the effective mass according to

$$G_E^* = F_1 - \tau \frac{m_N^*}{m_N} F_2 \quad (19)$$

$$G_M^* = F_1 + \frac{m_N^*}{m_N} F_2. \quad (20)$$

We use here the successful CC2 prescription of the electromagnetic nucleon current, that reproduces the experimental superscaling function [12]. Using the CC1 operator obtained through the Gordon reduction produces the same effects as in the RMF of ref. [12]. The same modification of form factors in the medium was explored in ref. [29], but the  $\psi^*$ -scaling was not investigated in that context. For the free Dirac and Pauli form factors,  $F_1$  and  $F_2$ , we use the Galster parametrization.

Note that our formalism generalizes the conventional SuSA formulae. In fact for  $M^* = 1$  we recover the SuSA results and definitions.

The factorization of Eq. (6) implies that the cross section in the RMF for nuclear matter also factorizes as the product of the scaling function times a single nucleon cross section. In this approach the scaling function is a parabola.

### The SuSAM\*

In the SuSAM\* approach we compute the cross section by using the above formulas, but replacing the scaling function (2) by a phenomenological one which we extract from the experimental data.

We start with the more than 2500 experimental ( $e, e'$ ) cross section data for  $^{12}\text{C}$  [30]. For every kinematical point we compute the corresponding experimental scaling function  $f_{\text{exp}}^*$

$$f_{\text{exp}}^* = \frac{\left( \frac{d\sigma}{d\Omega' d\epsilon'} \right)_{\text{exp}}}{\sigma_{\text{Mott}} (v_L r_L + v_T r_T)} \quad (21)$$

In ref. [26] we performed an analysis of the experimental scaling function for the bulk of data [30, 31] by plotting them against the scaling variable  $\psi^*$ . A large fraction of the data then collapses into a cloud with an asymmetrical shape as seen in Fig. 1. The cloud of data forms a thick band. The selection of data was made in ref. [26] by measuring the density of points clustered above a given threshold  $n$ , inside a circle of radius  $r = 0.1$ . The selection of data depends on the chosen value of  $n$ . In this work we use  $n = 25$ , meaning that we neglect all the points with less than 25 neighbours inside a circle of radius  $r = 0.1$ . The number of surviving data is around 1000. The thickness of the data cloud measures the small degree of scaling violation around the quasielastic peak. The neglected data correspond to inelastic excitations and low energy processes that highly violate scaling and

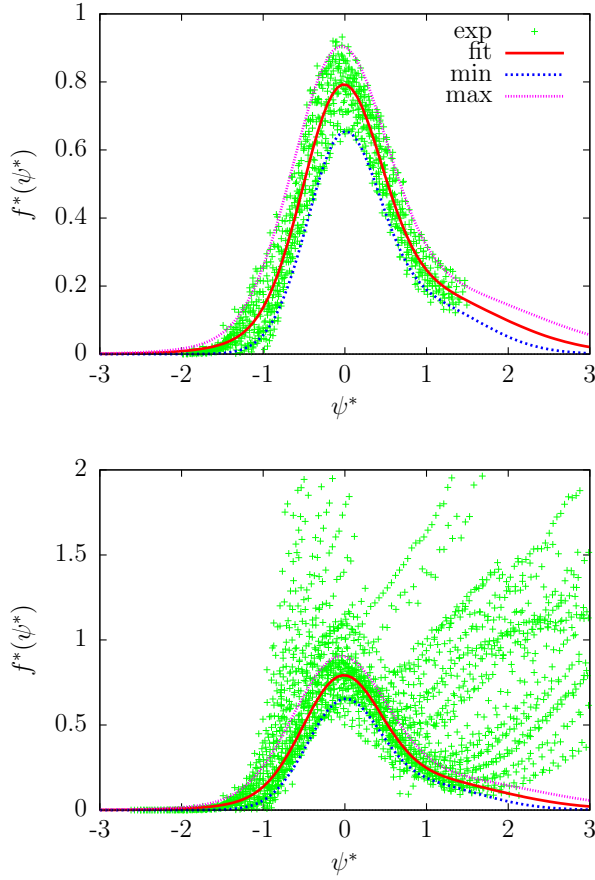


FIG. 1: Top panel: Phenomenological  $M^*$ -scaling function  $f^*(\psi^*)$  and its uncertainty band,  $f_{min}^* < f^* < f_{max}^*$ , for  $^{12}\text{C}$ , obtained from a fit to the experimental data. Only data with density  $n \geq 25$  inside a circle with radius  $r = 0.1$  have been included in the fit. Bottom panel: comparison of the present fit to the bulk set of world data. Data are from ref. [30–32]

	$a_1$	$a_2$	$a_3$	$b_1$	$b_2$	$b_3$
central	-0.0465	0.469	0.633	0.707	1.073	0.202
min	-0.0270	0.442	0.598	0.967	0.705	0.149
max	-0.0779	0.561	0.760	0.965	1.279	0.200

TABLE I: Parameters of our fit of the phenomenological scaling function central value,  $f^*(\psi^*)$ , and of the lower and upper boundaries (min and max, respectively).

cannot be considered quasielastic processes, as can be seen in the lower panel of Fig. 1.

In Fig. 1 we show also our new parametrization of the scaling function after a fit to the selected (quasielastic) experimental data. They are well described as a sum of two Gaussian functions

$$f^*(\psi^*) = a_3 e^{-(\psi^* - a_1)^2 / (2a_2^2)} + b_3 e^{-(\psi^* - b_1)^2 / (2b_2^2)} \quad (22)$$

The coefficients are given in table 1.

The lower and upper limits of the experimental data band have also been parametrized as sum of two Gaus-

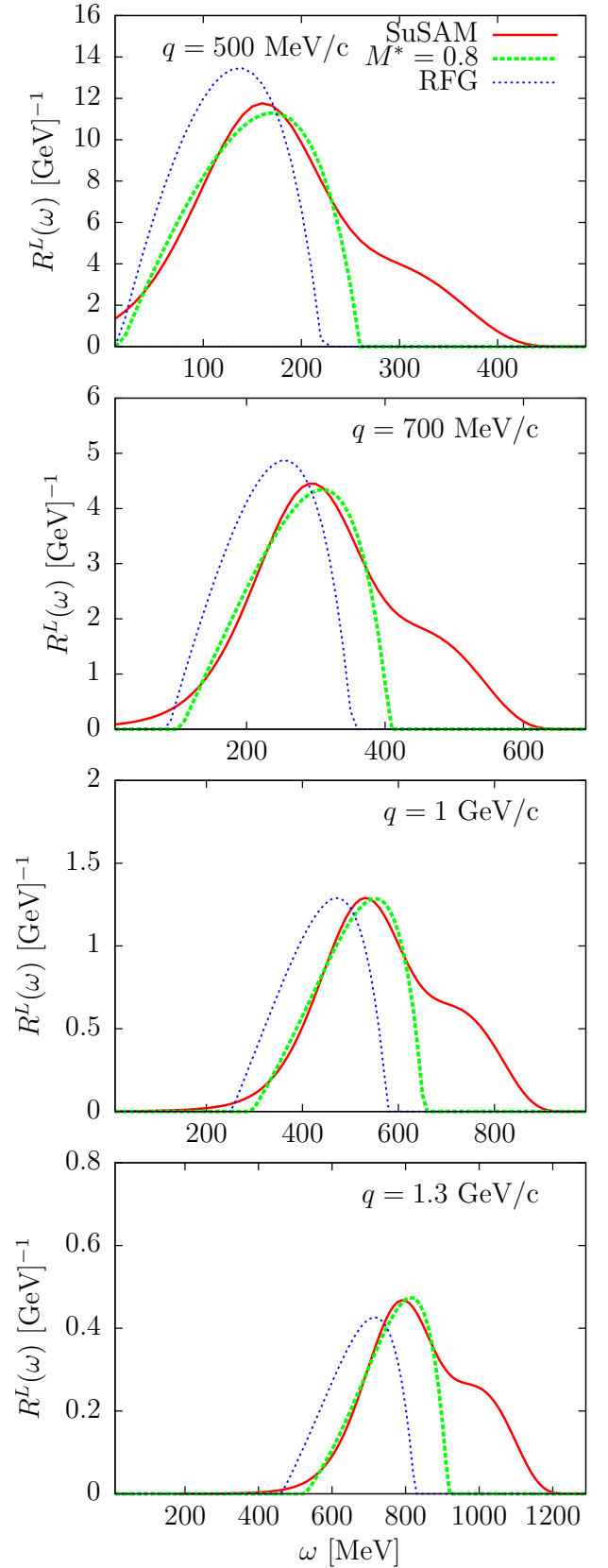


FIG. 2: Longitudinal response function of  $^{12}\text{C}$  in the SuSAM model, for several values of the momentum transfer. The relativistic Fermi gas results for effective mass  $M^* = 1$  and  $0.8$  are also shown. The Fermi momentum is  $k_F = 225 \text{ MeV}/c$ .

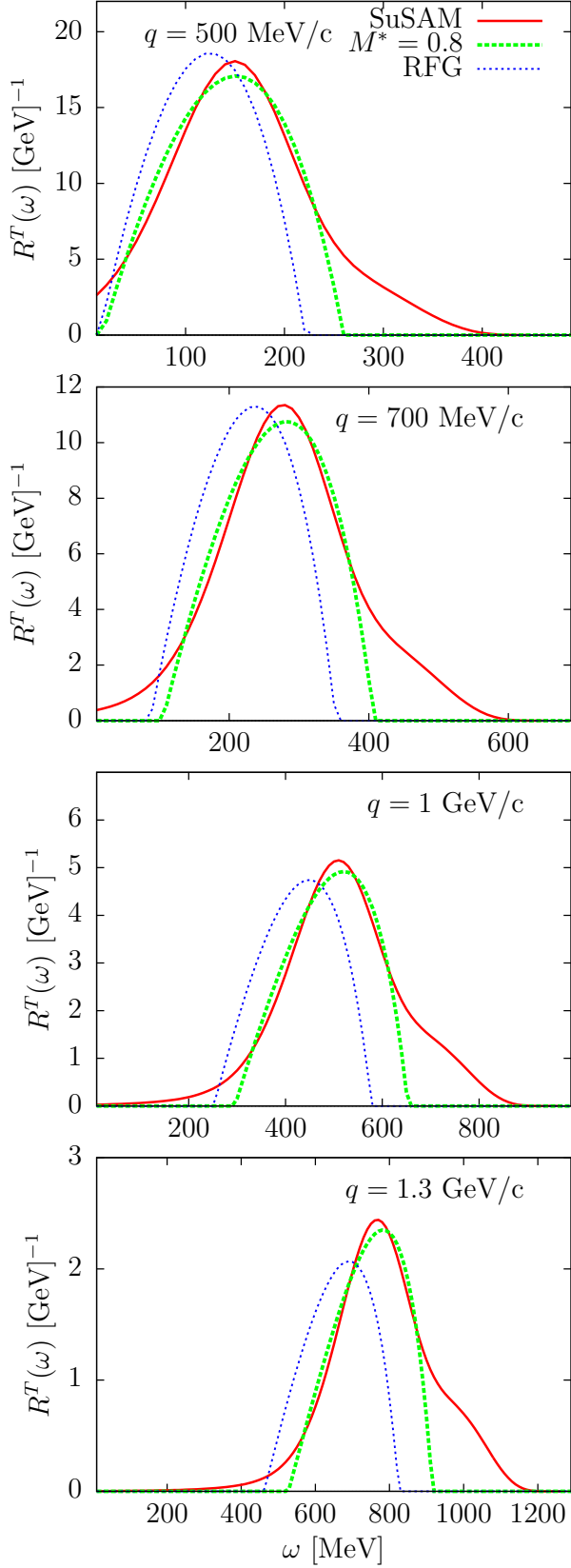


FIG. 3: Transverse response function of  $^{12}\text{C}$  in the SuSAM model, for several values of the momentum transfer. The relativistic Fermi gas results for effective mass  $M^* = 1$  and  $0.8$  are also shown. The Fermi momentum is  $k_F = 225$  MeV/c.

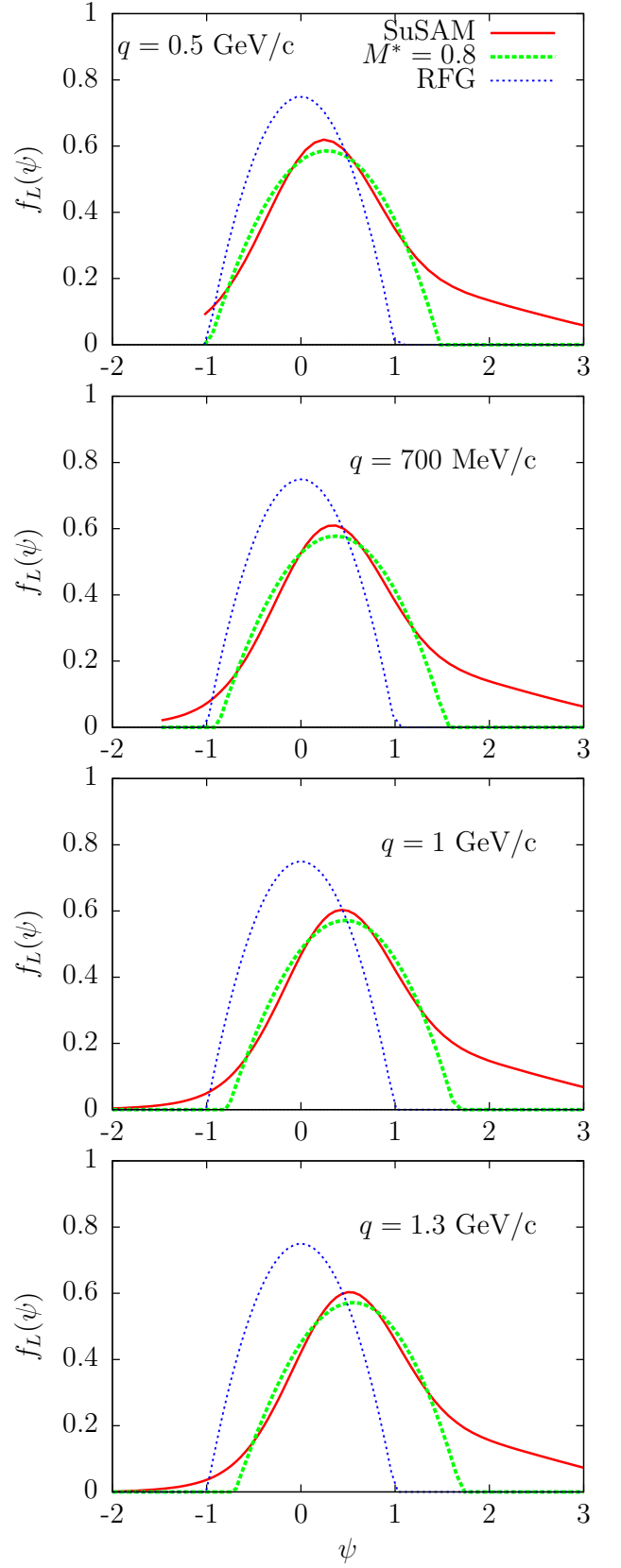


FIG. 4: Traditional longitudinal scaling function  $f_L(\psi)$  of  $^{12}\text{C}$  in the SuSAM model, for several values of the momentum transfer. The relativistic Fermi gas results for effective mass  $M^* = 1$  and  $0.8$  are also shown. The Fermi momentum is  $k_F = 225$  MeV/c.

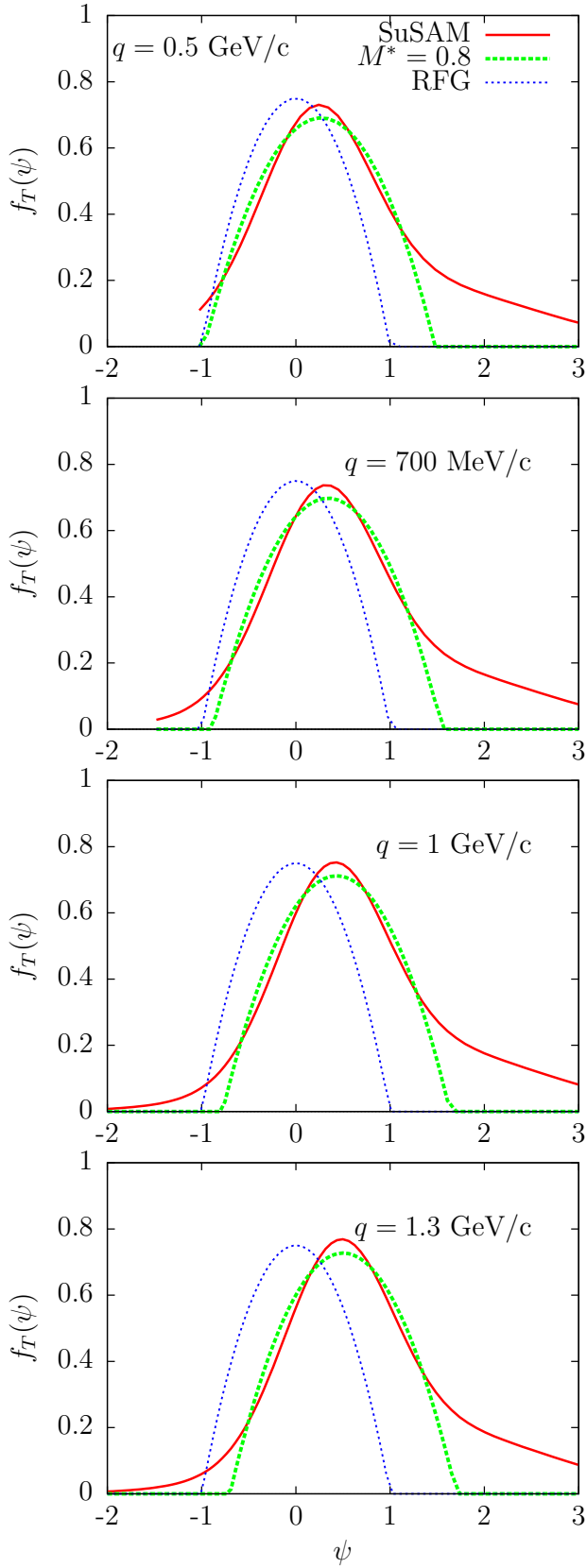


FIG. 5: Traditional transverse scaling function  $f_T(\psi)$  of  $^{12}\text{C}$  in the SuSAM model, for several values of the momentum transfer. The relativistic Fermi gas results for effective mass  $M^* = 1$  and  $0.8$  are also shown. The Fermi momentum is  $k_F = 225 \text{ MeV/c}$ .

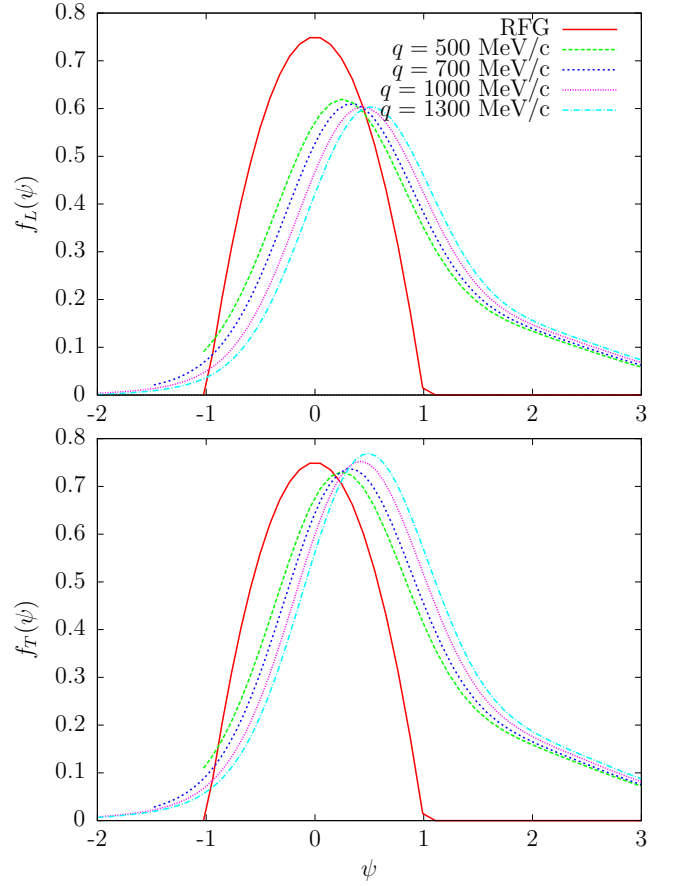


FIG. 6: Traditional scaling analysis of the longitudinal and transverse scaling functions of  $^{12}\text{C}$  in the SuSAM model, for several values of the momentum transfer. The universal relativistic Fermi gas scaling function is also shown for comparison

sians, with coefficients  $a_i^{min/max}$ ,  $b_i^{min/max}$ , given in table 1 as well.

Our phenomenological scaling function describes the center values of the selected data cloud and the average thickness. The thickness can be interpreted as a fluctuation produced by nuclear effects beyond the impulse approximation (finite size effects, short-range NN-correlations, long-range RPA, meson-exchange currents, virtual  $\Delta$  excitation, two-particle emission, final state interaction) [26].

## RESULTS

In this section we use the new phenomenological scaling function of the SuSAM\* model, given by eq. (22), to compute the response functions and cross section of  $^{12}\text{C}$  and the corresponding uncertainty band derived from the thickness of the fitted data set.

In figs 2 and 3 we show the longitudinal and transverse response functions for several values of the momentum



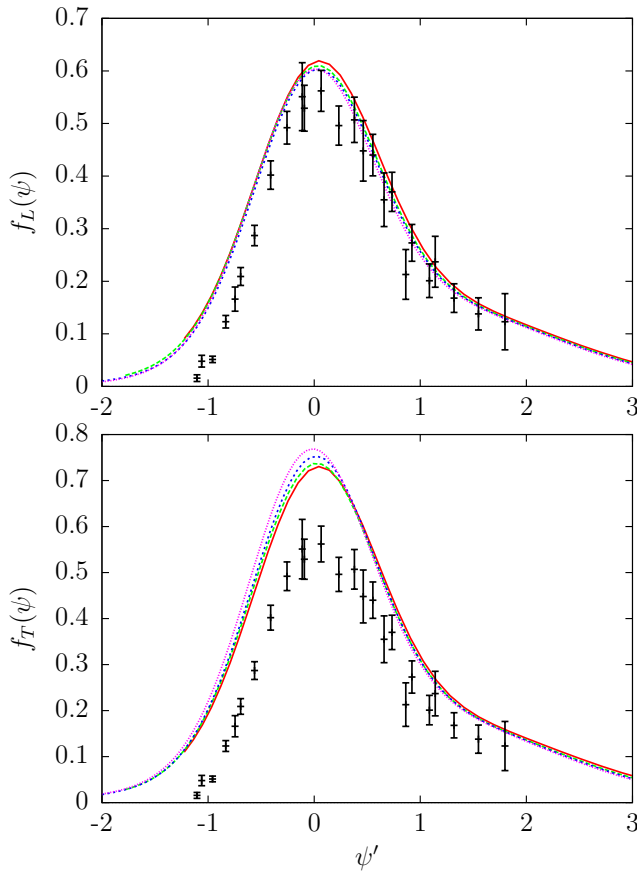


FIG. 7: Traditional scaling analysis of the longitudinal and transverse scaling functions of  $^{12}\text{C}$  in the SuSAM model, for several values of the momentum transfer. They are plotted as a function of the shifted variable  $\psi'$  so that the maximum in each curve is reached at  $\psi' = 0$ . For comparison we also plot the data of the longitudinal scaling function obtained from the experimental  $R_L(q, \omega)$  data in ref. [21].

transfer. They are compared to the free RFG and to the interacting RFG with  $M^* = 0.8$ . The effect of the effective mass is a shift of the responses to higher energies, because the position of the quasielastic peak is given by  $\omega = \sqrt{q^2 + m_N^{*2}} - m_N^*$ . Note that this shift gives the correct position of the quasielastic peak without need of introducing a separation energy parameter [27, 33]. In fact the position of the peak with the SuSAM\* model almost coincides with the RFG with  $M^* = 0.8$ .

The introduction of the phenomenological scaling function produces a prominent tail for high energy transfer, which extends much higher than the upper end of the RFG responses, which is more in accordance with the experimental data. This high end is a consequence of the maximum momentum for the nucleons in the Fermi gas, bound by the Fermi momentum, corresponding to  $\psi^* = 1$ . Since the data in Fig.1 extends above  $\psi^* = 1$ , this indicates the presence of final state interactions and also high momentum components in the nuclear wave function in the

ground state, which are thought to be caused by finite size effects and nuclear correlations [34, 35]. Another smaller tail appears for low energy also produced by nuclear effects.

The structure of the high energy tail is different in the longitudinal and transverse responses. The longitudinal response presents a prominent shoulder, which is not so prominent in the transverse one, although both responses have been calculated with the same phenomenological scaling function. Given that the scaling function does not present a similar shoulder, one can trace back its origin to the energy dependence of the single nucleon responses in the medium, that have been calculated with  $M^* = 0.8$ , see Eqs. (7–20).

In comparing the ratio between  $R_T$  and  $R_L$  from figs. 2 and 3 one can also observe an enhancement for the case  $M^* = 0.8$ . This is related with the known enhancement of the lower components in the relativistic spinor in the nuclear medium.

In Figs 4 and 5 we show the longitudinal and transverse scaling functions  $f_L(\psi)$  and  $f_T(\psi)$ , obtained from the response of Figs 2, 3, by dividing by the single nucleon responses with effective mass  $M^* = 1$ . These can be directly compared to the traditional SuSA scaling functions. They are plotted against the original scaling variable  $\psi$  for different values of  $q$ . It is apparent that they are almost independent on  $q$ . They are compared to the scaling function of the free RFG. The  $f_L(\psi)$  scaling function is smaller than the free one as in the case of the phenomenological SuSA scaling function. The  $f_T(\psi)$  scaling function is larger and almost of the same size as the free one, being this again a consequence of the enhancement of the transverse response function.

The  $\psi$ -scaling properties of the SuSAM\* model can be better observed in fig. 6. The scaling is only approximate as it happens with the RMF model. There is a shift with respect to the RFG parabola, which increases slightly with the momentum transfer. This increase is approximately linear. The enhancement of the transverse response also increases with  $q$  (bottom panel of Fig. 6).

In fig. 7 we compare the  $\psi$ -scaling function of our model with the experimental data of the longitudinal scaling function  $f_L(\psi)$  obtained in ref. [21]. The longitudinal scaling function is well reproduced, except a slight disagreement for low  $\psi'$ , because we fit the cross section and not  $R_L$ . The transverse scaling function in our model is evidently larger than the experimental  $f_L(\psi')$  in an amount about 20 %, similar to the RMF results of [12].

In figs. 8–13 we show the predictions of our model for the  $(e, e')$  cross section compared to the experimental data. Our global description is quite acceptable given the few parameters of the SuSAM\* model. A large fraction of the data fall inside our uncertainty band. In fact, most of the data used to perform the fit, and displayed in Fig. 1 (top) are inside our prediction bands by construction.

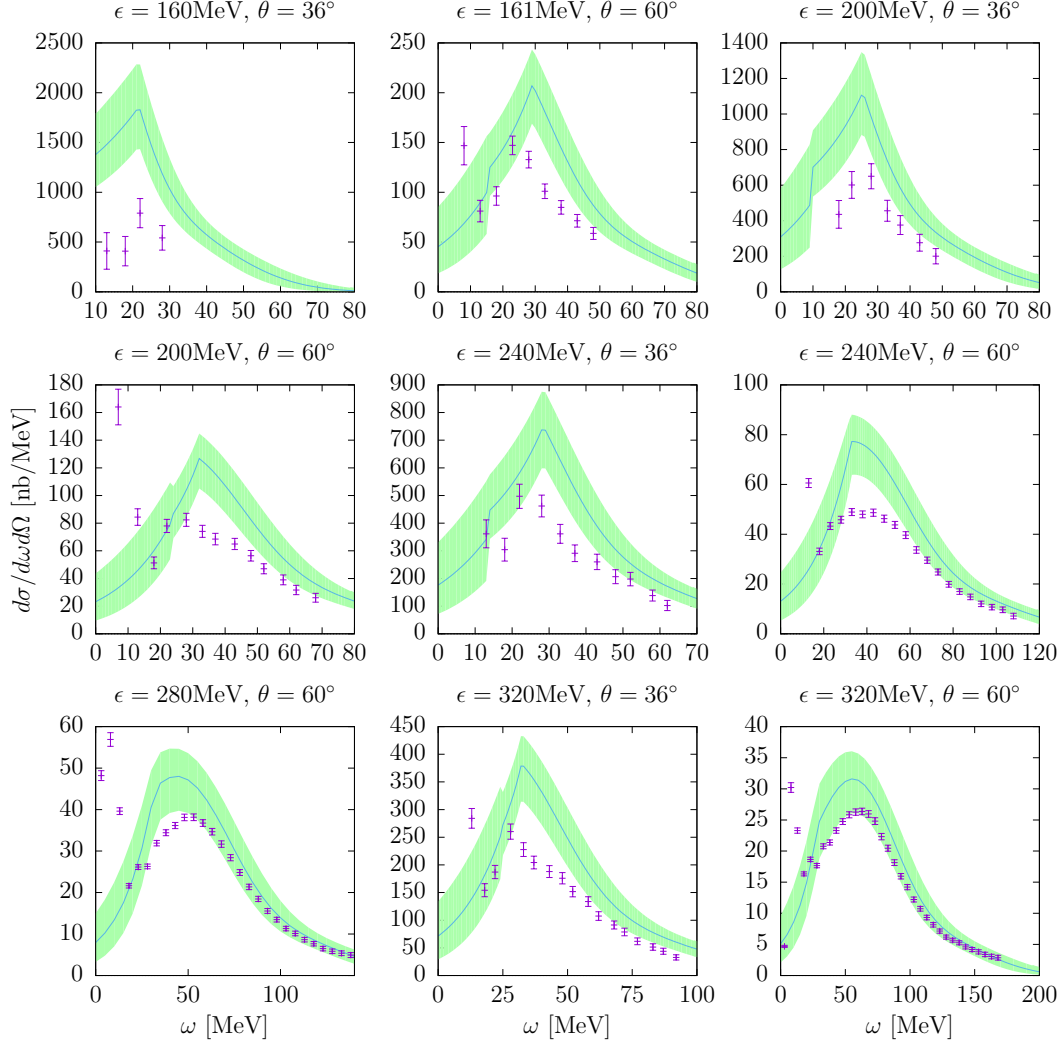


FIG. 8: SuSAM predictions and uncertainty bands for the quasielastic ( $e, e'$ ) cross section for several kinematics compared to the experimental data.

The data that lie outside our prediction bands are those clearly in the inelastic or deep region and those corresponding to low excitation energy, and therefore break  $\psi^*$ -scaling because they fall outside the quasielastic region defined in fig. 1 (top).

## CONCLUSIONS

In this paper we have investigated a novel scaling approach based on a new scaling variable  $\psi^*$  extracted from the scaling properties of the RMF model in nuclear matter. Within this model we have obtained a phenomenological scaling function  $f^*(\psi^*)$  from the inclusive ( $e, e'$ ) reaction data off  $^{12}\text{C}$ , after a selection procedure of the quasielastic subset of data. This new phenomenological scaling function has been parametrized as the sum of two Gaussians. Additionally, an uncertainty band has been

assigned to the phenomenological scaling function from the dispersion of the data set around the central value.

With this scaling function we have calculated the longitudinal and transverse response functions and the conventional scaling functions of the SuSA model. Our model contains the enhancement of the transverse components of the electromagnetic current by construction. This confirms the RMF interpretation of the enhancement of the transverse response in terms of the relativistic modification of the lower components of the nucleon spinors in the medium, that we encode with the effective nucleon mass reduction of  $M^* = 0.8$ .

Finally we have computed the differential quasielastic cross section with an uncertainty band generated by the scaling function thickness and compared to the world  $^{12}\text{C}(e, e')$  data, with a reasonable description of around one thousand data, which thus can be tagged as truly quasielastic.



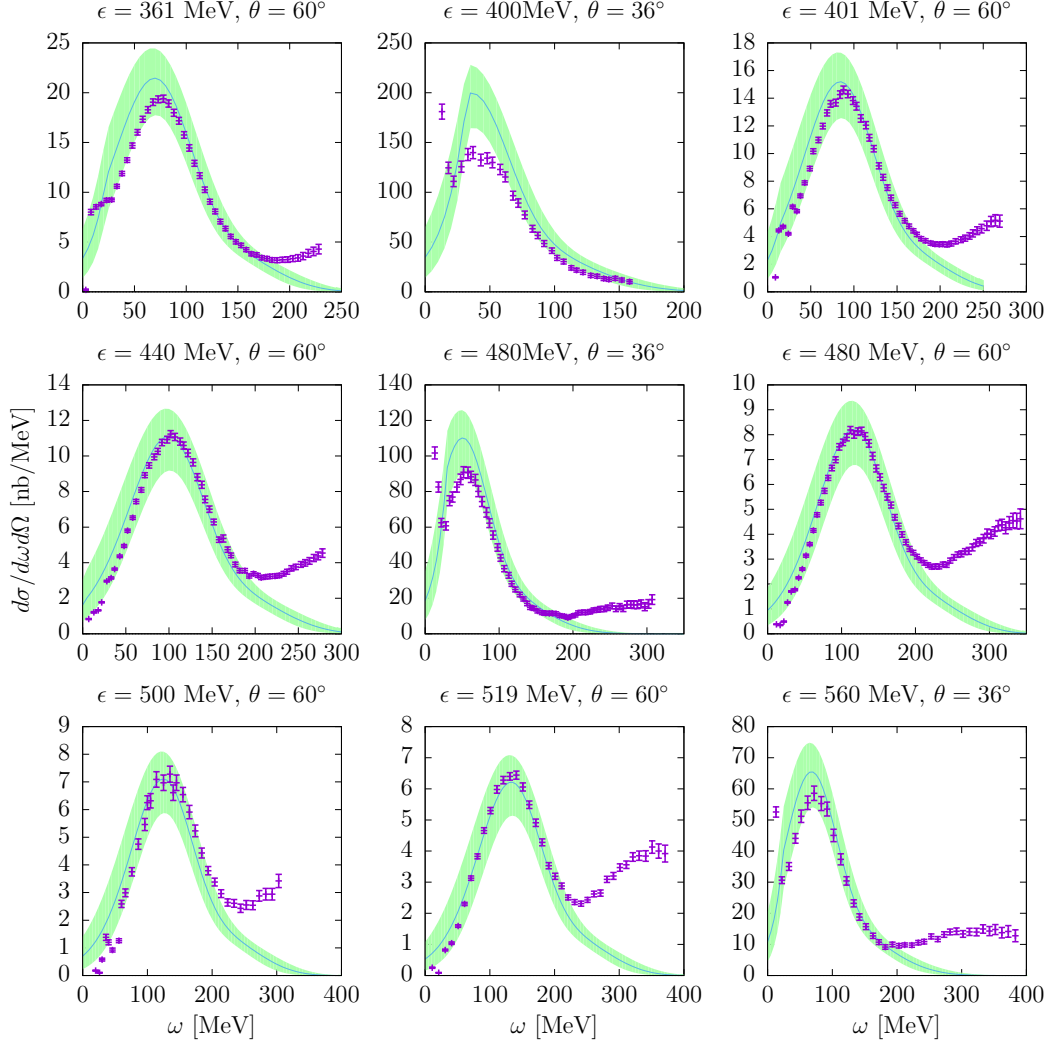


FIG. 9: SuSAM predictions and uncertainty bands for the quasielastic ( $e, e'$ ) cross section for several kinematics compared to the experimental data.

This model predicts a quasielastic cross section directly from the data without any theoretical assumption, besides the requirements of gauge invariance, relativity and scaling, which determines the values of the relativistic effective mass and the Fermi momentum. The rest of nuclear effects contributing to the quasielastic reaction, have been encoded into the parametrized scaling function  $f^*(\psi^*)$  within an uncertainty band. Any model aiming to describe the quasielastic cross section at intermediate energies should lie inside the SuSAM\* uncertainty band. Therefore, our scaling function parametrization provides a novel test for theoretical scaling studies. This imposes constraints over the transverse enhancement, additional to those imposed by the longitudinal scaling function in the SuSA model. In line with the current revival of electron scattering this model can be easily extended to provide tight constraints in quasielastic neutrino scattering.

## ACKNOWLEDGEMENTS

This work is supported by Spanish DGI (grant FIS2014-59386-P) and Junta de Andalucía (grant FQM225). I.R.S. acknowledges support from the Ministerio de Economía y Competitividad (grant Juan de la Cierva-Incorporación).

---

\* Electronic address: amaro@ugr.es

† Electronic address: earriola@ugr.es

‡ Electronic address: ruizsig@ugr.es

- [1] V Lyubushkin et al. (NOMAD Collaboration), Eur. Phys. J. C 63 (2009), 355.
- [2] A. Aguilar-Arevalo *et al.* (MiniBooNE Collaboration), Phys. Rev. D **81**, 092005 (2010).
- [3] A. Aguilar-Arevalo *et al.* (MiniBooNE Collaboration),

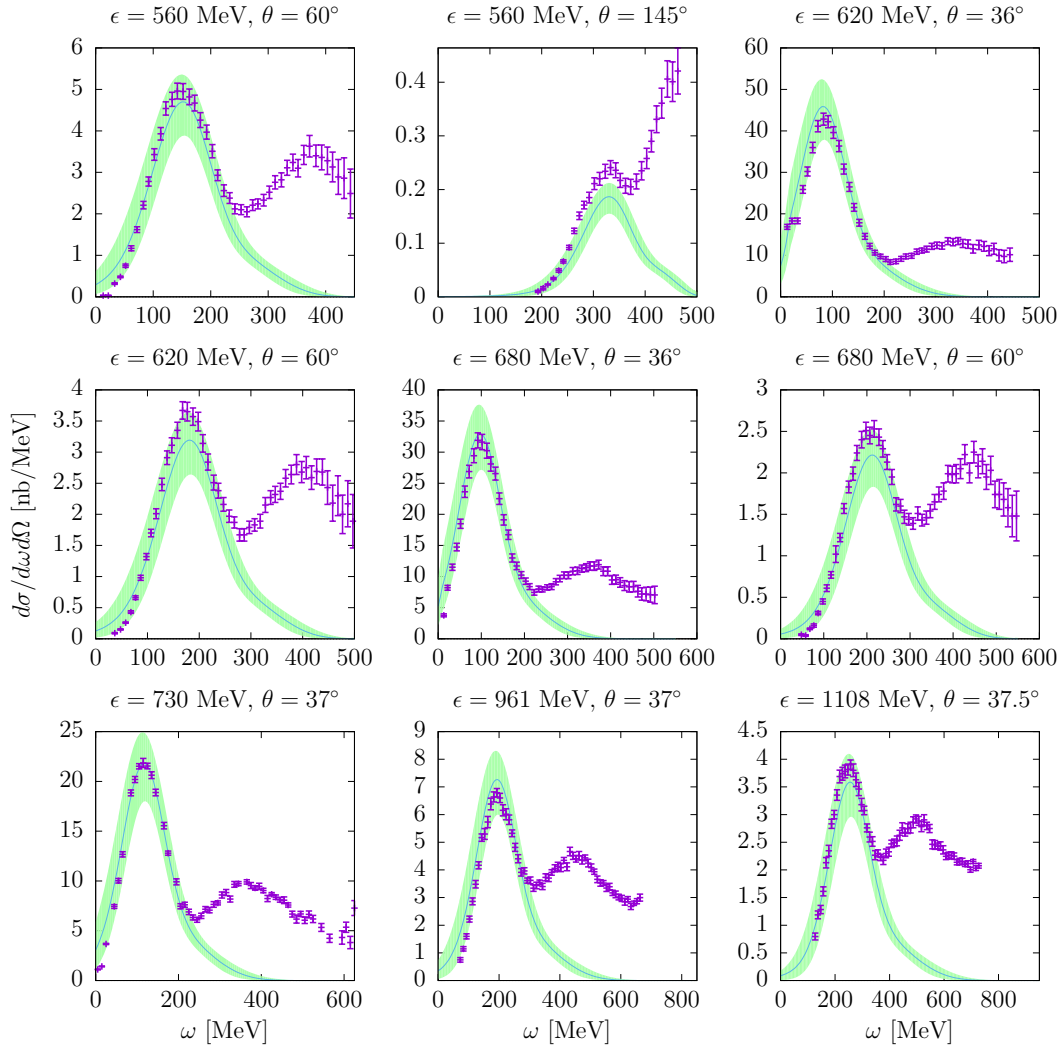


FIG. 10: SuSAM predictions and uncertainty bands for the quasielastic ( $e, e'$ ) cross section for several kinematics compared to the experimental data.

- Phys. Rev. D **88**, 032001 (2013).
- [4] G.A. Fiorentini *et al.* (MINERvA Collaboration) Phys. Rev. Lett. **111**, 022502 (2013).
- [5] K. Abe *et al.*, (T2K Collaboration), Phys. Rev. D **87**, 092003 (2013).
- [6] A. Lovato, S. Gandolfi, J. Carlson, Steven C. Pieper, R. Schiavilla, Phys.Rev.Lett. **117** (2016) 082501.
- [7] A. M. Ankowski, O. Benhar, M. Sakuda, Phys. Rev. D **91**, 033005 (2015).
- [8] N. Rocco, A. Lovato, O. Benhar, Phys.Rev.Lett. **116** (2016) 192501.
- [9] V. Pandey, N. Jachowicz, T. Van Cuyck, J. Ryckebusch and M. Martini, Phys. Rev. C **92**, no. 2, 024606 (2015).
- [10] J. E. Amaro, M. B. Barbaro, J. A. Caballero, T. W. Donnelly and A. Molinari, Phys. Rept. **368**, 317 (2002).
- [11] J. E. Amaro, M. B. Barbaro, J. A. Caballero, T. W. Donnelly and C. Maieron, Phys. Rev. C **71**, 065501 (2005).
- [12] J. A. Caballero, J. E. Amaro, M. B. Barbaro, T. W. Donnelly and J. M. Udias, Phys. Lett. B **653**, 366 (2007).
- [13] J. M. Udias, J. A. Caballero, E. Moya de Guerra, J. E. Amaro and T. W. Donnelly, Phys. Rev. Lett. **83**, 5451 (1999).
- [14] A. Bodek, M.E. Christy, and B. Coopersmith, Eur. Phys. Jou. C **74**, 3091 (2014).
- [15] A. Gil, J. Nieves and E. Oset, Nucl. Phys. A **627** (1997) 543.
- [16] I. Ruiz Simo, J. E. Amaro, M. B. Barbaro, A. De Pace, J. A. Caballero and T. W. Donnelly, arXiv:1604.08423 [nucl-th].
- [17] J. Nieves, J.E. Sobczyk, arXiv:1701.03628 [nucl-th].
- [18] T. W. Donnelly and I. Sick, Phys. Rev. Lett. **82**, 3212 (1999).
- [19] T. W. Donnelly and I. Sick, Phys. Rev. C **60**, 065502 (1999).
- [20] W.M. Alberico, A. Molinari, T.W. Donnelly, E. L. Kronenberg, and J.W. Van Orden, Phys Rev. C **38** (1988) 1801.
- [21] C. Maieron, T. W. Donnelly and I. Sick, Phys. Rev. C **65**, 025502 (2002).
- [22] J. E. Amaro, M. B. Barbaro, J. A. Caballero, T. W. Donnelly, A. Molinari, I. Sick, Phys. Rev. C **71**, 015501 (2005).

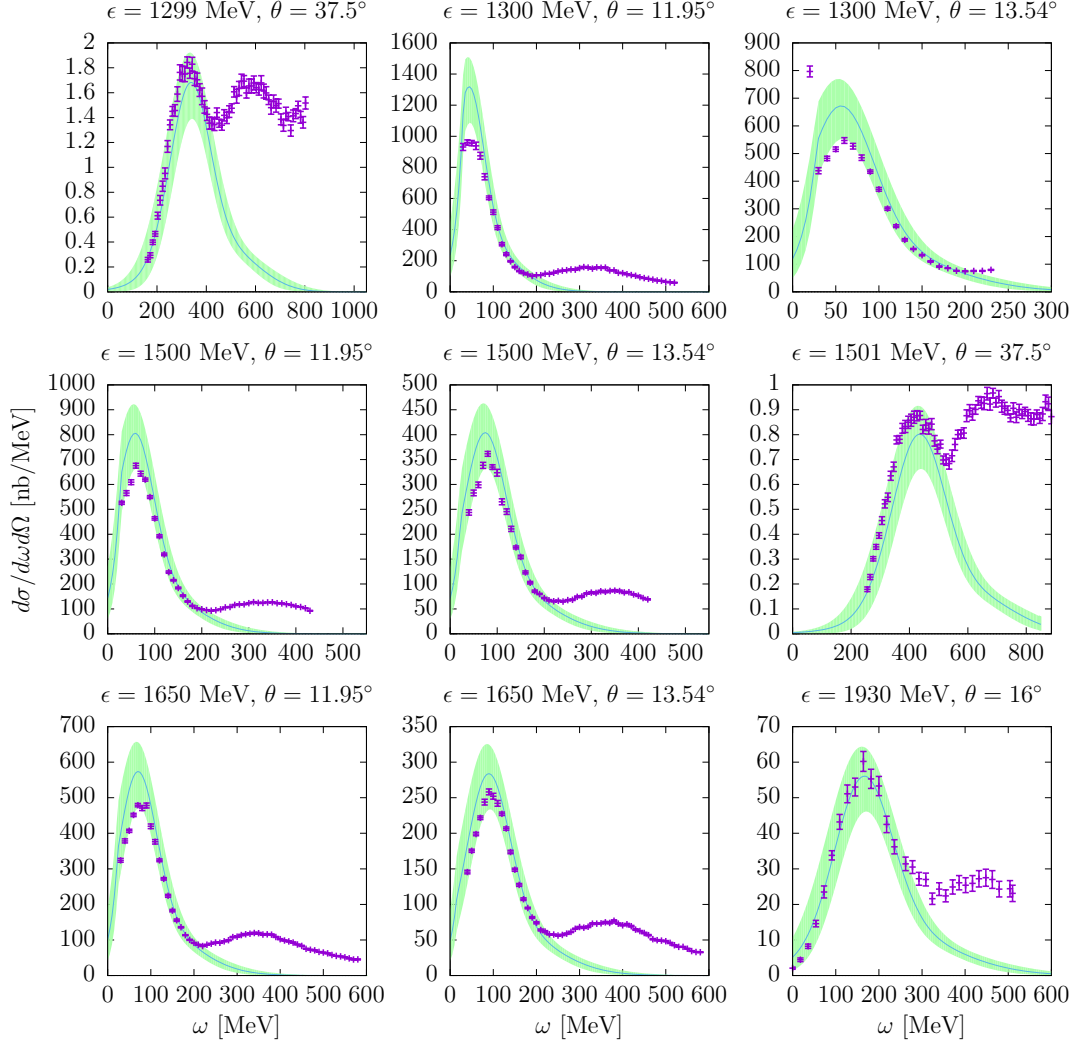


FIG. 11: SuSAM predictions and uncertainty bands for the quasielastic ( $e, e'$ ) cross section for several kinematics compared to the experimental data.

- [23] C.J. Horowitz, D.P. Murdock, and B.D. Serot, in *Computational Nuclear Physics Vol. 1*, Springer-Verlag, Berlin 1991.
- [24] T. De Forest, Nucl. Phys. A **392**, 232 (1983).
- [25] R. Gonzalez-Jimenez, G.D. Megias, M.B. Barbaro, J.A. Caballero, and T.W. Donnelly, Phys. Rev. C **90**, 035501 (2014).
- [26] J. E. Amaro, E. Ruiz Arriola and I. Ruiz Simo, Phys. Rev. C **92**, no. 5, 054607 (2015)
- [27] R. Rosenfelder, Ann. Phys. (N.Y.): 128, 188 (1980)
- [28] B.D. Serot, and J.D. Walecka, Adv. Nucl. Phys. **16** (1986) 1.
- [29] M.B. Barbaro, R. Cenni, A. De Pace, T.W. Donnelly, A. Molinari, Nucl. Phys. A **643** (1998) 137.
- [30] O. Benhar, D. Day, and I. Sick, <http://faculty.virginia.edu/qes-archive/>
- [31] O. Benhar, D. Day and I. Sick, arXiv:nucl-ex/0603032.
- [32] O. Benhar, D. Day, and I. Sick, Rev Mod Phys. **80** (2008) 189
- [33] K. Wehrberger, Phys. Rep. **225** (1993) 273.
- [34] R. B. Wiringa, R. Schiavilla, S. C. Pieper and J. Carlson, Phys. Rev. C **89**, no. 2, 024305 (2014)
- [35] I. Ruiz Simo, R. N. Perez, J. E. Amaro and E. Ruiz Arriola, arXiv:1612.06228 [nucl-th].

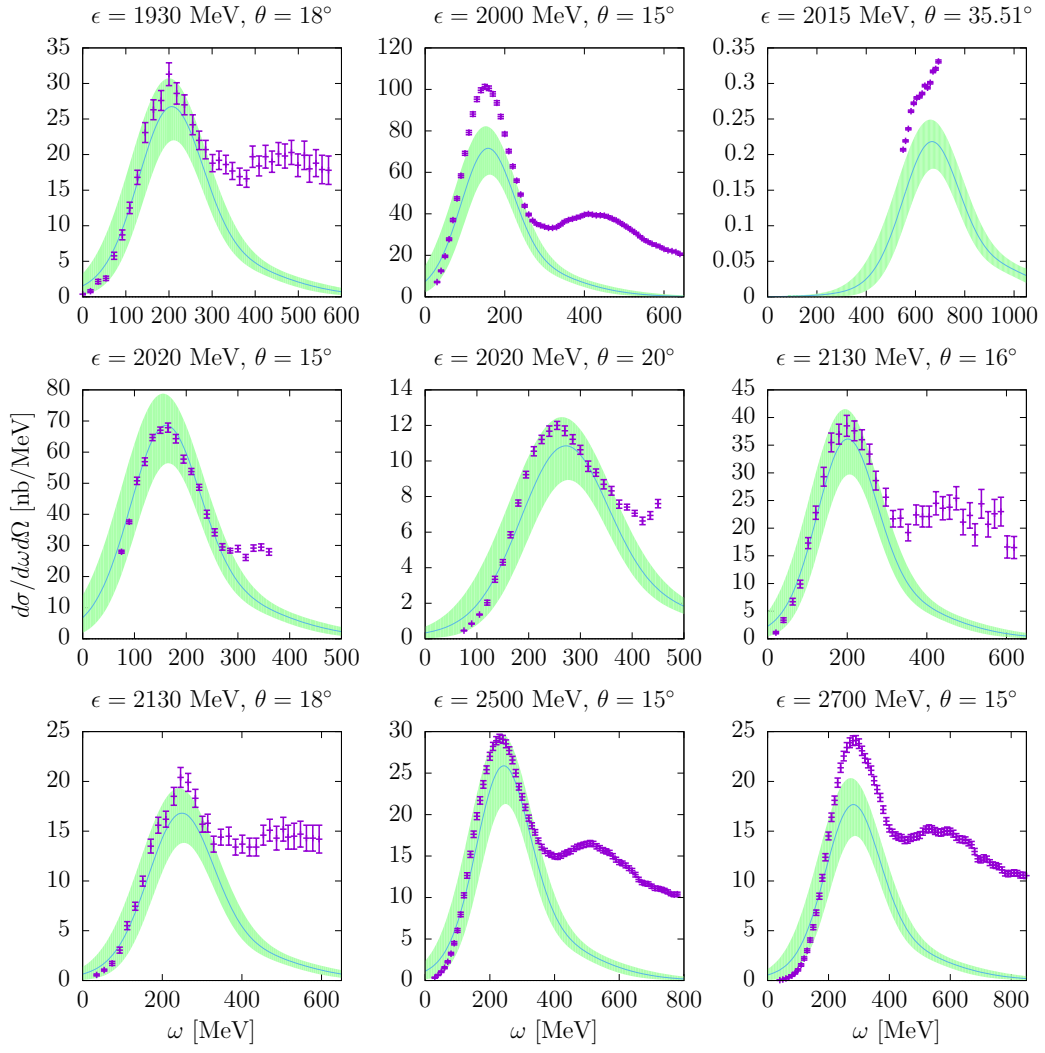


FIG. 12: SuSAM predictions and uncertainty bands for the quasielastic ( $e, e'$ ) cross section for several kinematics compared to the experimental data.

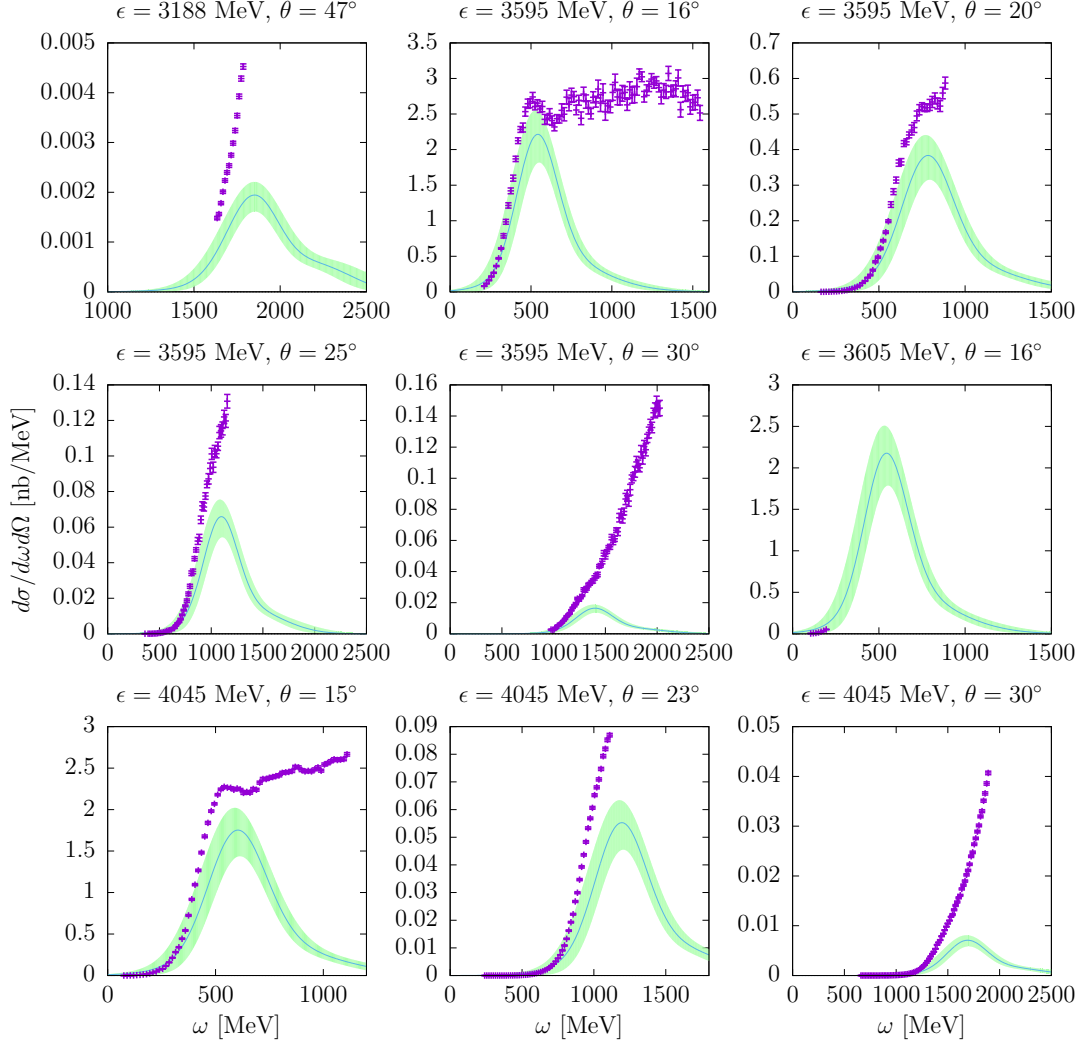


FIG. 13: SuSAM predictions and uncertainty bands for the quasielastic ( $e, e'$ ) cross section for several kinematics compared to the experimental data.